



OPEN ACCESS

EDITED BY

Olivier Lambert,
Institut royal des Sciences naturelles de
Belgique, Belgium

REVIEWED BY

Vivian De Buffrénil,
Muséum National d'Histoire Naturelle,
France
Mark Uhen,
George Mason University, United States

*CORRESPONDENCE

Svitozar Davydenko,
✉ yurgenvorona@ukr.net
Pavel Gol'din,
✉ pavelgoldin412@gmail.com

RECEIVED 17 February 2023

ACCEPTED 27 April 2023

PUBLISHED 09 May 2023

CITATION

Davydenko S, Tretiakov R and Gol'din P
(2023), Diverse bone microanatomy in
cetaceans from the Eocene of Ukraine
further documents early adaptations to
fully aquatic lifestyle.
Front. Earth Sci. 11:1168681.
doi: 10.3389/feart.2023.1168681

COPYRIGHT

© 2023 Davydenko, Tretiakov and
Gol'din. This is an open-access article
distributed under the terms of the
[Creative Commons Attribution License
\(CC BY\)](https://creativecommons.org/licenses/by/4.0/). The use, distribution or
reproduction in other forums is
permitted, provided the original author(s)
and the copyright owner(s) are credited
and that the original publication in this
journal is cited, in accordance with
accepted academic practice. No use,
distribution or reproduction is permitted
which does not comply with these terms.

Diverse bone microanatomy in cetaceans from the Eocene of Ukraine further documents early adaptations to fully aquatic lifestyle

Svitozar Davydenko^{1*}, Roman Tretiakov² and Pavel Gol'din^{1*}

¹I.I. Schmalhausen Institute of Zoology, National Academy of Sciences of Ukraine, Kyiv, Ukraine, ²The Institute of Traumatology and Orthopedics, National Academy of Medical Sciences of Ukraine, Kyiv, Ukraine

Basilosauridae, fully aquatic archaeocetes from the Eocene, had osteosclerotic or pachyosteosclerotic structure of ribs and, sometimes, other bones. Such a structure is far different from osteoporotic-like bones of modern cetaceans. A microanatomical and histological study was conducted on axial and limb skeleton of several basilosaurid specimens assigned to the genus *Basilotritus*, from Bartonian (late middle Eocene) deposits of Ukraine, remarkable for its pachyostotic bones. The postcranial skeleton of these specimens is a complex mosaic of diverse types of bone structure, which include pachyosteosclerotic, osteosclerotic and cancellous elements. The vertebrae have a pachyostotic layered cortex reaching its greatest thickness in the lumbar region. This cortex was strongly vascularized, and its layered structure is due to concentric circles mostly made by longitudinal vascular canals, in addition to cyclical growth lines. Heavy bones are concentrated in the dorsal and ventral areas. Swollen distal ends of thoracic ribs are interpreted as serving as ballast in the ventral area, as also previously proposed for *Basilosaurus cetoides*. Cortical bone tissue in vertebrae and ribs showed signs of intensive resorption and remodeling. This indicates the use of the axial skeleton not only for buoyancy control but also possibly for calcium and phosphorus recycling.

KEYWORDS

Eocene, bone remodeling, paleohistology, microstructure, postcranial skeleton, pachyosteosclerosis, Pelagiceti, Basilosauridae

1 Introduction

Several tetrapod lineages transitioned to aquatic lifestyle and gained numerous evolutionary adaptations to life in water. Two main types of histological adaptations of bone tissue can be found in secondarily aquatic tetrapods. The first one is an increase of bone density and mass through either hyperplasia of the periosteal cortex (pachyostosis) or compaction of endosteal bone (osteosclerosis) resulting from different ontogenetic processes (reviewed in: Ricqlès and De Buffrénil, 2001; Houssaye and Buffrénil, 2021). Pachyostosis and osteosclerosis, as well as the combination of these conditions, pachyosteosclerosis, occur in different parts of the postcranial skeleton of many unrelated taxa of extant and extinct aquatic mammals and reptiles (Buffrénil et al., 1990; Buffrénil et al., 2010; Hayashi et al., 2013; Houssaye et al., 2015; Nuñez Demarco et al., 2018; Dewaele et al., 2019; Dewaele et al., 2022). Such a bone

microstructure is often interpreted as helping to reduce body buoyancy in bottom dwelling and/or shallow marine species. A well-known example of this anatomy is the extensively pachyosteosclerotic skeleton of extinct and modern sirenians (Buffrénil and Schoevaert, 1989; Buffrénil et al., 2010).

The second type of aquatic adaptations implies reduction of bone mass and density (osteoporotic-like state) through the intensification of bone resorption. Osteoporotic postcranial bones are typical of derived marine reptiles and modern cetaceans: they are associated with a pelagic lifestyle (Buffrénil and Schoevaert, 1988; Buffrénil and Mazin, 1990; Houssaye et al., 2014; Scheyer et al., 2014). However, there are examples of very different histological adaptations in closely related taxa (Klein et al., 2016) or even at different ontogenetic stages of the same species (Wiffen et al., 1995; George et al., 2016).

Cetaceans changed the type of their bone microstructure adaptations during their early evolution. Stem semi-aquatic cetaceans, Pakicetidae, Ambulocetidae, Remingtonocetidae and Protocetidae, had osteosclerotic ribs and limb bones (Gray et al., 2007; Madar, 2007; Thewissen et al., 2007; Houssaye et al., 2015; Houssaye et al., 2016). Meanwhile, the earliest Pelagiceti (fully aquatic cetaceans), developed pachyosteosclerosis: it was found in the postcranial skeleton of Basilosauridae and in ribs of the earliest mysticete *Mystacodon selenensis* (Muizon et al., 2019) with pestle-like distal ends. Like *M. selenensis*, most of basilosaurids had swollen ribs and moderately osteosclerotic forelimb bones (Buffrénil et al., 1990; Houssaye et al., 2015). However, there were large-sized cetaceans, such as *Basilosaurus*, which had pachyostotic cortex in their torso (i.e., posterior thoracic, lumbar and anterior caudal) vertebrae (Houssaye et al., 2015). Moreover, there were several cetaceans in the Eocene, known from Africa, North and South America and Europe (Uhen, 1999; Uhen et al., 2011; Gol'din and Zvonok, 2013; Gol'din et al., 2014b; van Vliet et al., 2020; Gingerich et al., 2022), which shared the same morphotype: robust skeletons with pachyosteosclerotic ribs, vertebrae and scapulae. Most of these animals are known only from highly fragmentary finds scattered across the globe. This led to some taxonomical confusion. Several nominal taxa sharing this anatomy were described and recombined or synonymized, such as genera *Pachycetus*, *Platyosphys*, *Basilotritus* and *Antaetetus*, and also *Eocetus* (later recombined as "*Eocetus*", *Basilotritus*, *Platyosphys* and *Pachycetus*) *wardii* (Van Benden, 1883; Kellogg, 1936; Uhen, 1999; Gol'din and Zvonok, 2013; van Vliet et al., 2020; Gingerich et al., 2022), while others were reported as unnamed cetaceans (Uhen et al., 2011). These genera and their morphological similarity were reviewed by Gingerich, Amane and Zouhri (2022). However, due to the fragmentary nature of the specimens and, most likely, homoplasy in postcranial traits shared by cetaceans of this morphotype (Davydenko et al., 2021), the conclusions of that revision are still debated and pending phylogenetic analysis. Meanwhile postcranial anatomy of this morphotype is highly unusual for cetaceans, and only several forms from the Miocene of Paratethys (baleen whales of the family Cetotheriidae and the toothed whale *Pachyacanthus*) developed similar structures in their postcranial skeleton (Gol'din et al., 2014a; Dewaele et al., 2022). Bone histology that underlies this rare morphotype is a subject of special

interest, since it shows the earliest steps of cetacean adaptations to a fully aquatic way of life.

Two specimens of basilosaurids, previously reported as *Basilotritus* sp. (Gol'din and Zvonok, 2013; Gol'din et al., 2014a), from the Eocene deposits of Ukraine provide unique information on bone macro- and microanatomy of this morphotype. In this study we provide the analysis of the inner bone structure and histology of the mandible, vertebrae, ribs, scapula, pelvis and fore- and hind limb bones of these whales from evolutionary, biomechanical and ontogenetic perspectives.

2 Material and methods

Thirteen postcranial bones (Supplementary Table S1, Supplementary Figure S2) and a mandible fragment were taken for thin section preparation and CT scanning from the specimen referred to as *Basilotritus* sp. from the Kyiv Formation (Upper Lutetian to Bartonian, Middle Eocene) of Nahirne, Ukraine (approximate geographic coordinates 49°05'N, 33°08'E) (Gol'din and Zvonok, 2013; Gol'din et al., 2014b). Parts of this skeleton are housed in collections of the Geological Museum of Taras Shevchenko National University of Kyiv, Ukraine (GMNTSNUK) and Academician V.A. Topachevsky Paleontological Museum of the National Museum of Natural History of the National Academy of Sciences of Ukraine (NMNH-P). History of this collection and arguments for attributing all the Nahirne bones to a single individual and to the genus *Basilotritus* were provided in a previous work dedicated to the anatomy of this specimen (Gol'din et al., 2014b).

Another specimen of the same or closely related taxon (here referred to as *Basilotritus* sp.) comes from the coast of the Pyvykha Mt., Ukraine (approximate geographic coordinates 49°11'N, 33°07'E) and is held in the Hradyzk Local History Museum, Hradyzk, Ukraine (HLHM). Bones of this specimen (Supplementary Table S1, Supplementary Figure S3) were found recently washed from the coastal sediments. Based on the sediments covering some of the bones, this basilosaurid comes from the Kyiv Formation, like the Nahirne specimen. Also, a single caudal vertebra NMNH-P OF-1970 (referred as well to *Basilotritus* sp.) comes from the same locality (Gol'din and Zvonok, 2013) and it could belong to the same specimen, based on its preservation state, size and ontogenetic state. All the bones of the Pyvykha specimen are compatible in size and suture fusion stage, and there are no duplicate elements, so all the Pyvykha bones likely belong to a single individual.

Both Nahirne and Pyvykha specimens share the same postcranial skeletal morphotype, with thick cortex on the surface of posterior thoracic and lumbar vertebrae, swollen (pachyosteosclerotic) thoracic ribs, anteroposteriorly elongated transverse processes of lumbar vertebrae and presence of two cones of cancellous bone within the centra of lumbar vertebrae. No diagnostic morphological differences were found between the postcranial bones of the two specimens, so they are tentatively re-identified as belonging to the same genus or even species. However, this assignment should be used with caution, due to the absence of more diagnostic cranial and dental remains from the Pyvykha specimen.

Additionally, the CT scan of thoracic vertebrae of the holotype of the Bartonian *Basilotritus uheni*, specimen NMNH-P OF-2096 (Gol'din and Zvonok, 2013), was used for the comparative analysis of the inner microstructure of postcranial bone.

In total, 19 disarticulated bones and bone fragments from all the mentioned collections were examined (Table 1). Body length calculation was based on the linear regressions of the vertebral column length derived from the length of the longest vertebra from the posterior lumbar or anterior caudal region; moreover, skull length was derived from the centrum width of a cervical vertebra C3 or C4 (Davydenko et al., 2021). Seventeen bones were CT scanned at the Institute of Traumatology and Orthopedics, National Academy of Medical Sciences of Ukraine. The fossils were scanned with a Philips Brilliance 16-slice CT scanner. The same settings of the tube were used for all the specimens (voltage 120 kV; 120 mA). Virtual sections were visualized with the RadiAnt DICOM Viewer software (Medixant, 2021). Inner parts of the bones are free from mineralized matrix due to the significant contrast between cavities and bone as seen on CT scans and visual absence of the filling matrix in fresh fractures on cancellous bone.

Thin sections of the bones were manually prepared according to the standard procedure (Lamm, 2013). The thickness of the sections varied between 30 and 50 μm . Thin sections were examined under natural and polarized light, with an Olympus BX51 microscope (x40–x200). Sections were photographed with a Nikon D40 camera. Compactness index for the rib was calculated using the Bone Profiler (version 4.5.8) software (Girondot and Laurin, 2003).

Microanatomical structure of the bones was described with a terminology adapted from work dedicated to general bone histology of vertebrates (Francillon-Vieillot et al., 1990) and previous articles describing inner microstructure of archaeocete bones (Buffr enil et al., 1990; Gray et al., 2007).

3 Results

3.1 Ontogenetic state of the specimens

The Pyvykha specimen is suggested to represent the youngest individual in our sample. It includes bones (ribs and vertebrae) showing signs of a young individual age. There are three annuli in the inner structure of the ribs (here we use the term “annuli” following Buffr enil and Quilhac, 2021). Only cervical and anterior caudal vertebrae have partially fused epiphyses, but no signs of suture fusion were found in thoracic or lumbar vertebrae fragments. This sequence of vertebrae epiphysis fusion is typical of modern cetaceans (Kato, 1988; Galatius and Kinze, 2003; Moran et al., 2015). The Pyvykha specimen is the smallest individual in our sample. Its body length, tentatively estimated from the dimensions of the longest (caudal) vertebra and the cervical vertebra (Davydenko et al., 2021), was about 7 m.

The Nahirne specimen is older, with five to six annuli visible in its ribs. Its body length, estimated from the dimensions of the longest (lumbar) vertebra and the cervical vertebra, was about 8 m. Vertebral epiphyses are partially fused in cervical vertebrae only.

Physical immaturity, as inferred from the fusion state of vertebral epiphyses, along with the relatively large size of

Pyvykha and Nahirne specimens and the heavily worn teeth in the latter, might be indicative of pedomorphosis, as discussed in the previous study of the Nahirne specimen (Gol'din et al., 2014b).

The holotype of *Basilotritus uheni* is an adult individual close to physical maturity: its posterior thoracic vertebrae (presumably T7–T9) have completely or almost completely fused epiphyses (Gol'din and Zvonok, 2013). Therefore, *B. uheni* OF-2096 is the most mature specimen in this research. However, it is unclear if it is conspecific to the other specimens.

3.2 Inner anatomy

3.2.1 Cervical vertebrae (NMNH-P CS 48–50, HLHM EC 01)

All the CT scanned cervical vertebrae have epiphyses incompletely (partially) fused with centra. The cervical vertebrae mostly consist of cancellous bone (Supplementary Figure S2C). A relatively thick cortex (7–10 mm) can be found only on the ventrolateral surface of C7 (CS 50) and at the base of the pedicles of the neural arch (Figure 1C).

3.2.2 Thoracic vertebrae (NMNH-P OF-2096, HLHM EC 01)

The inner core of the centrum is composed of cancellous bone and in lateral view it has the shape of a ventrally concave cylinder (Figure 1A). Also, inner parts of the pedicles of the neural arch consist of cancellous bone (Figure 1B). The ventral part of the centrum, rib facets, pedicles of neural arch, spinal process and postzygapophyses are surrounded by thick cortex (maximum thickness is about 20 mm) radially penetrated by irregular canals (Figure 1B).

3.2.3 Lumbar vertebra (NMNH-P Ngr-12)

The outer surface of the centrum, the bases of transverse processes and the pedicles of the neural arch are covered with a thick compact cortex showing at least six layers that are visible on CT-scans in the best-preserved parts (Figure 2A). Radial vascular canals penetrate the layered cortex, and these canals reach the outer surfaces of the centrum where they are seen as numerous vascular pits. These openings, earlier described as “pock marks”, were noticed as a diagnostic trait for several taxa of Eocene cetaceans (Uhen, 1999; Gol'din and Zvonok, 2013; van Vliet et al., 2020; Gingerich et al., 2022). The thickest cortex (30 mm) is in the middle third of the centrum, whereas at the anterior and posterior margins of the centrum the cortex is relatively thin (5–10 mm). The inner core of the centrum is hourglass-shaped: it is composed by two cones of cancellous bone tapering towards each other in the midline area (Figure 2B), from which the cancellous cores of transverse processes are transversely extended (Figure 2A). Cortical bone is much thicker on the dorsal surface of the bases of transverse processes (23 mm) than on the ventral surface (15 mm). The neural arch pedicles consist only of compact cortical bone, without cancellous inner cores. *Basilosaurus cetoides* was previously reported to have a similarly thickened cortex of the lumbar vertebrae (Houssaye et al., 2015). However, cortical bone on *B. cetoides* vertebrae is thinner, especially at the base of transverse processes.

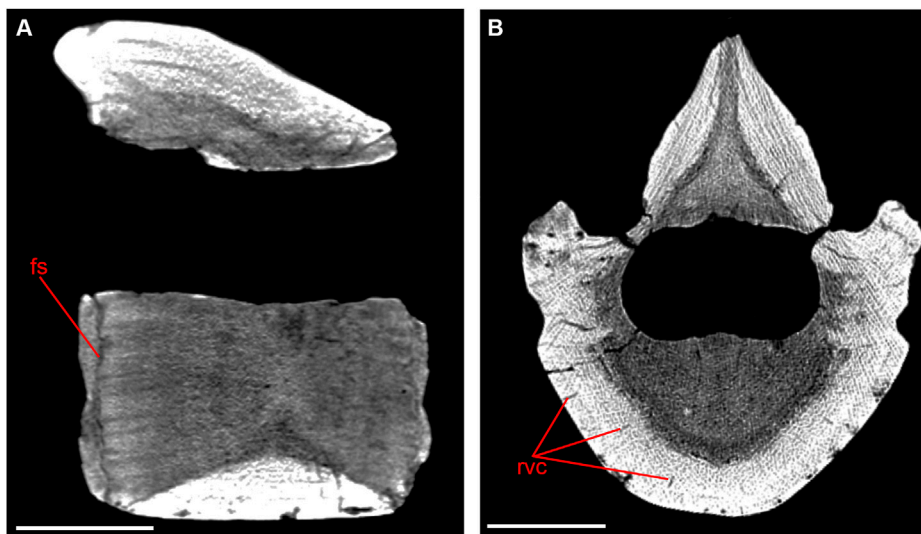


FIGURE 1
CT-scans of thoracic vertebra T7 of *Basilotritus uheni* (NMNH-P OF-2096). (A) Longitudinal cross section. (B) Transverse cross section of T7. Abbreviations: fs, fused suture; rvc, radial vascular canals. All scale bars are 50 mm.

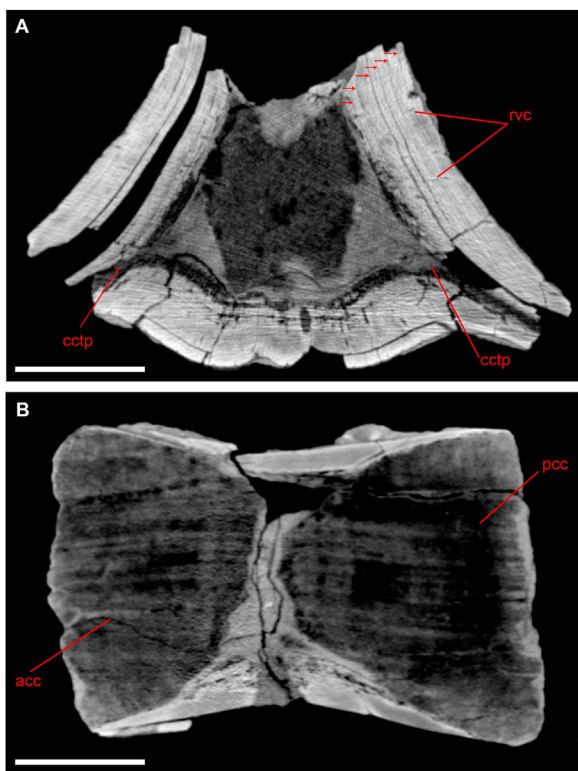


FIGURE 2
CT-scans of lumbar vertebra of *Basilotritus* sp. (Nahirne specimen, NMNH-P Ngr-12). (A) Transverse cross section. Visible longitudinal vascular canals distributed in circular rows are marked by arrows. (B) Longitudinal cross section. Abbreviations: acc, anterior cone of cancellous bone; cctp, cancellous core of transverse process; pcc, posterior cone of cancellous bone; rvc, radial vascular canals. All scale bars are 50 mm.

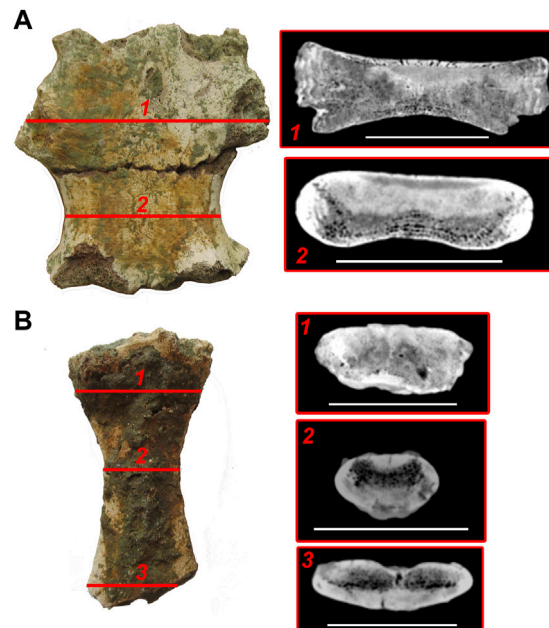


FIGURE 3
CT-scans of sternum elements of *Basilotritus* sp. (Nahirne specimen). (A) inner structure of the mesosternal element 2 (GMTSNUK 15/8). (B) inner structure of the xiphisternum (NMNH-P CS 44). Numbered lines correspond to respective transverse cross sections. All scale bars are 50 mm.

3.2.4 Anterior caudal vertebra (NMNH-P OF-1970)

Most of the outer surface of the vertebra is eroded, but some areas of the transverse cross-section are covered with a very thin (2–3 mm) cortex devoid of distinct layers ([Supplementary Figure](#)

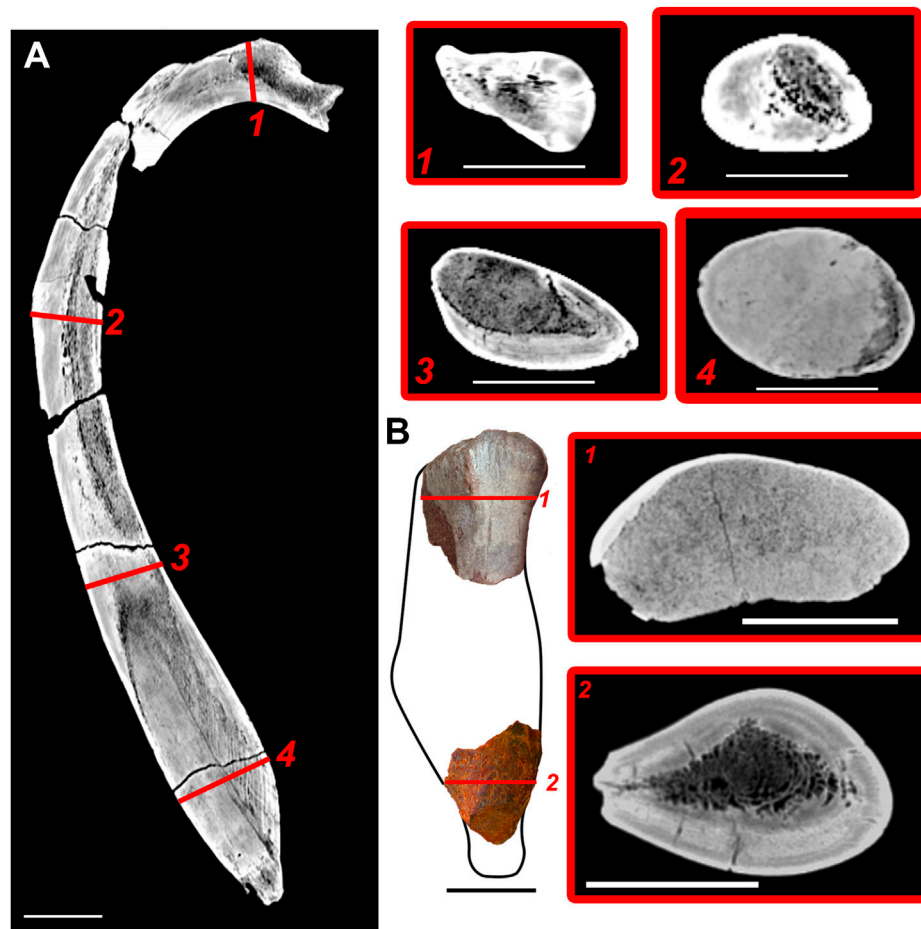


FIGURE 4

CT-scans of a rib (Nahirne specimen) and humerus (Pyvykha specimen) of *Basilotritus* sp. (A) longitudinal CT-scan of the thoracic rib (GMTSNUK 15/9). (B) CT-scans of proximal and distal fragments of the humerus (HLHM EC 01). Numbered lines correspond to respective transverse cross sections. All scale bars are 50 mm.

S3C). The inner core of the centrum is similar to the core of the lumbar vertebra NMNH-P Ngr-12. Both epiphyses are present and fused with the centrum. Suture lines are barely visible with the naked eye, but well distinguishable on CT-scans (Supplementary Figure S3D).

3.2.5 Mesosternal element 2 (GMTSNUK 15/8)

This bone almost entirely consists of spongy bone. There is a thin plate of compact cortex (4 mm) on the dorsal side of the anterior portion of the bone (Figure 3A). This plate is penetrated by numerous canals. The middle part of the mesosternal element is denser, and there is compact bone 10 mm thick on its dorsal side. The lateral walls of the bone are thin and consist of compact, layered bone also penetrated by canals.

3.2.6 Xiphisternum (NMNH-P CS 44)

The anterior end of the xiphisternum consists of cancellous bone with small, reduced intertrabecular spaces and irregular erosion cavities (Figure 3B). This inner structure smoothly changes into the midshaft of the bone, where separate intertrabecular spaces become better visible on virtual sections. Two zones of cortical bone are seen

in the periosteal area in the middle part of the xiphisternum: the thicker one (10 mm) on the ventral side of the bone and the thinner one (5 mm) on the dorsal side. There are three barely visible layers in the ventral cortical area. This area is pierced by vascular canals. At the bifurcated posterior end of the xiphisternum (Figure 3B), the dorsal cortical area is thinner (2 mm), so the cancellous bone is as thick as the compact bone in this area.

3.2.7 Thoracic rib (GMTSNUK 15/9)

The inner structure of the rib is highly variable along the bone shaft (Figure 4A). The proximal virtual section shows a middle core of spongy bone surrounded by a layered compact cortex. There are thick trabeculae and large intertrabecular spaces in the middle core. A similar structure is observed in the middle part of the rib diaphysis, but the spongy medulla is located on the medial side of the rib rather than in its centre. A similar asymmetry was previously documented for other basilosaurids: the medulla of ribs of *Basilosaurus isis* is also located on the medial side of the section (Houssaye et al., 2015), whereas in *Basilosaurus cetoides* and *Zygorhiza kochii* the cortex is much thicker on the medial side, so the medulla is situated laterally (Buffrénil et al., 1990). The structure of

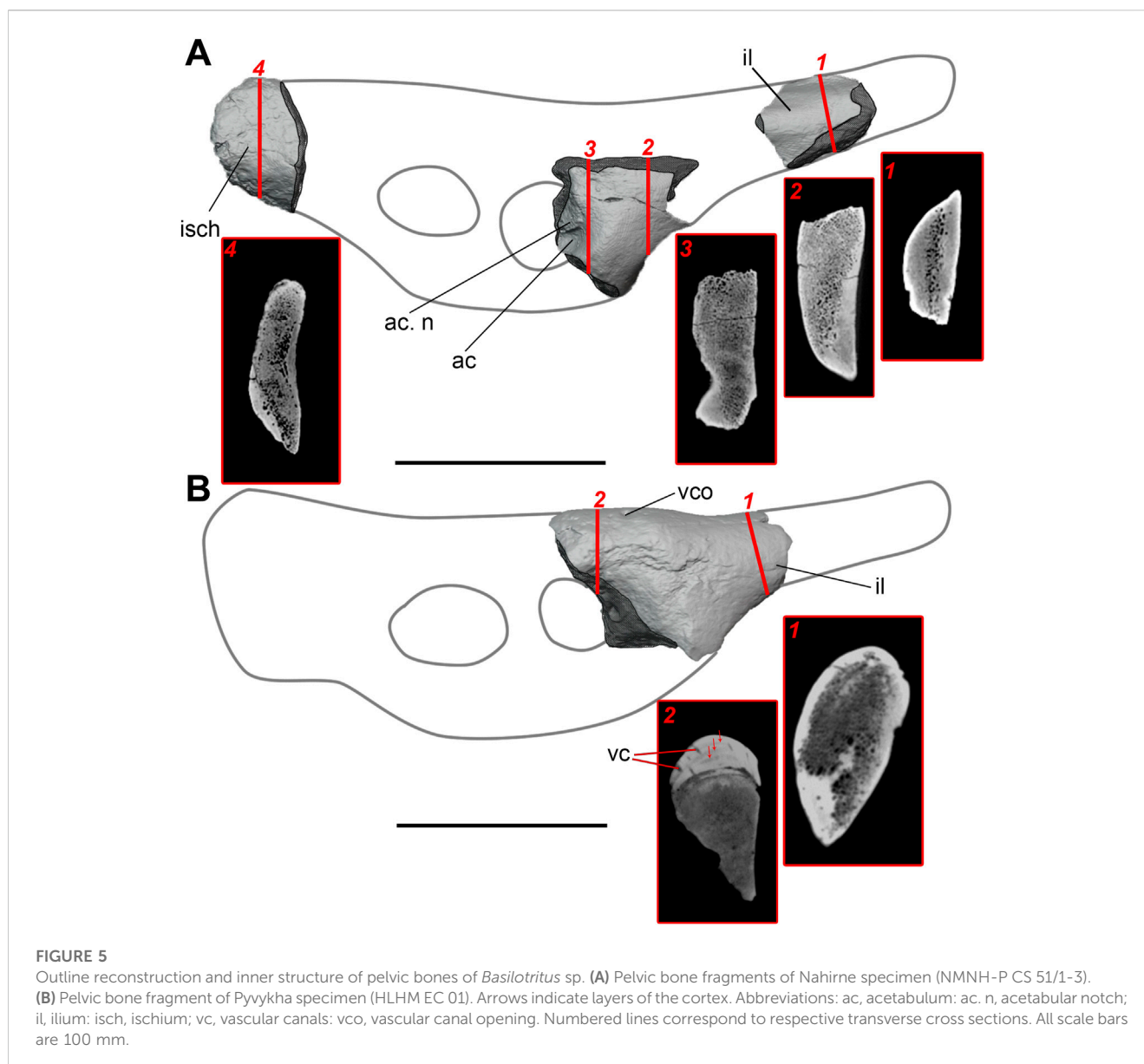


FIGURE 5

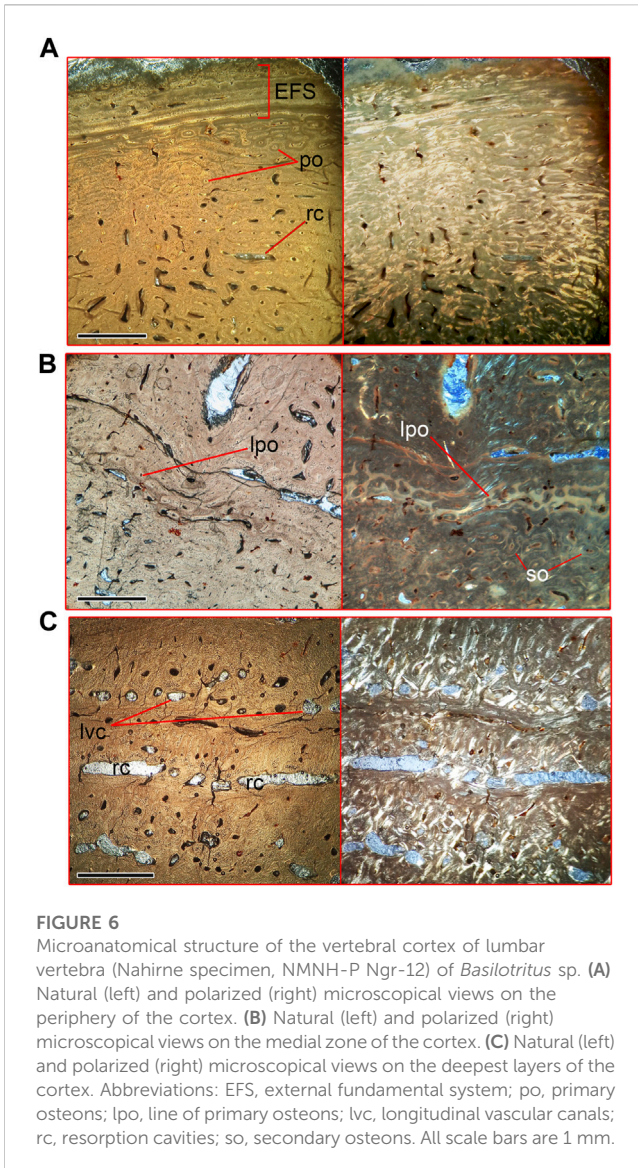
Outline reconstruction and inner structure of pelvic bones of *Basilotritus* sp. (A) Pelvic bone fragments of Nahirne specimen (NMNH-P CS 51/1-3). (B) Pelvic bone fragment of Pyvykha specimen (HLHM EC 01). Arrows indicate layers of the cortex. Abbreviations: ac, acetabulum; ac. n, acetabular notch; il, ilium; isch, ischium; vc, vascular canal; vco, vascular canal opening. Numbered lines correspond to respective transverse cross sections. All scale bars are 100 mm.

the medulla is different in the distal swollen portion of the rib: trabeculae are much denser and thicker, intertrabecular spaces are smaller, and lacunae are not seen (except for the boundary between medulla and cortex). Distally, the dense medulla occupies most of the bone. It is located at the anterior (rather than medial) margin of the rib, and the layered cortex is situated posterior to it. There are five or six well distinguishable but disturbed annuli (Supplementary Figure S2O), which are believed to be annual growth layers in many mammals (Klevezal, 1996), and resorption cavities in the compact bone. The most distal swelling of the rib consists almost entirely of enlarged medullar core with thick trabeculae. This core is surrounded by very thin (2–3 mm) cortex. The compactness index (CI) of the midshaft of the thoracic rib is 0.94 (Supplementary Figure S2O), as measured on the thin section prepared from the fragment of another thoracic rib of this specimen (NMNH-P CS 52, Supplementary Figure S2G). Generally, inner structure of the thoracic rib of *Basilotritus* is

similar to that of *B. isis*, differing in the slightly denser midshaft: CI is 0.94 in *Basilotritus* sp. vs. 0.88 in *B. isis* (Houssaye et al., 2015).

3.2.8 Humerus (HLHM EC 01)

The proximal part of the humerus (Figure 4B1) almost entirely consists of spongy bone with a dense trabecular network and small, numerous intertrabecular spaces. The thickest cortex is situated along the anterior margin of the bone. The distal fragment has a thick circular cortex (about 15 mm); medullar area of this fragment contains spongy bone with thinner trabeculae and large intertrabecular spaces (Figure 4B2). The medullar area partially extends into the deltopectoral crest. Compactness index of cross-section of the distal fragment is 0.81. Such a high density without a swelling of the bone indicates that the distal part of the humerus is osteosclerotic. Cross-section of the distal fragment of *Basilotritus* humerus is similar to that of *B. isis*, while a cancellous proximal part is similar to a proximal cross section of *Dorudon atrox* (Houssaye et al., 2015).



3.2.9 Proximal phalanx (NMNH-P CS 45)

This phalanx mostly consists of spongy bone tissue with numerous longitudinally elongated intertrabecular spaces. The spongy area is surrounded by very thin (1 mm), compact periosteal bone (Supplementary Figure S2N).

3.2.10 Innominate (NMNH-P CS 51/1-3)

The gross anatomy of the pelvic bone fragments is similar to that of the pelvis of “*Basilotritus*” (or “*Pachycetus*”) *wardii* (Uhen, 1999). In the inner structure, the innominate mostly consists of a loose spongiosa with thick trabeculae and large intertrabecular spaces. Two strata of compact bone, without any distinct layers and vascular canals, are located on the ventromedial side of the ilium base and the ventrolateral side of the deepest preserved part of the acetabulum (Figure 5A). The iliac process has a spongy core, elongated in dorsoventral direction, and the lateral and medial areas are made of dense non-layered compact bone. The ischium fragment has a similar inner structure, but the lateral and medial areas of compact bone are thinner.

3.2.11 Innominate (HLHM EC 01)

The preserved fragment, 126 mm long (Figure 5B), has a completely preserved dorsal margin that displays a pachyosteosclerotic bulging just above the acetabulum. Several openings of vascular canals are seen on that bulging. In the inner structure, a single dense area is seen on the ventral side of the bone, and the large pachyosteosclerotic swelling is dorsal to the acetabulum. The latter consists of an extremely dense compact cortex with several layers (Figure 8B). These layers are penetrated by numerous vascular canals.

3.3 Bone histology

3.3.1 Vertebral cortex

Compact cortical bone of lumbar vertebrae (a thin section in a cortex fragment of specimen NMNH-P Ngr-12 was prepared) can be subdivided into three areas (Figure 6, Supplementary Figure S4). The peripheral area is composed of a woven-parallel complex with irregular primary osteons. There are sparse and randomly placed resorption cavities in this area, without traces of remodeling. Four closely spaced lines of arrested growth (LAG) are seen in the periosteal zone (Figure 6A), forming the external fundamental system (EFS). A thin plate of woven bone tissue with small primary osteons is seen externally to the outer growth line, suggesting continuing periosteal growth. A line consisting of several rows of tightly packed primary osteons, surrounded by avascular woven bone tissue, separates the middle area of the cortex from the peripheral area (Figure 6B). The middle area contains scarce secondary osteons (Figure 6B) and numerous longitudinal vascular canals distributed in circular rows (Figure 6C). The third, deepest, area of the cortex is a well-ordered structure of circular canals, which is disturbed by intensive remodeling and numerous resorption cavities (Figure 6C). The cancellous bone is situated medial to the third area of cortex.

3.3.2 Thoracic rib (NMNH-P CS 52)

There are no EFS or any growth marks in the periosteal area. It is composed of parallel-fibered bone tissue and primary osteons. Four to six annuli, composed of parallel-fibered tissue, are placed in the cortex. There are two to four rows of primary osteons between neighboring annuli (Figure 7A). This area is disturbed by resorption, which prevents precise annulus counting. The deepest area of the cortex consists of woven-fibered bone tissue and evenly distributed secondary osteons. Medullar area of the rib is mostly filled by trabeculae, thickened by increased deposit of endosteal bone with numerous traces of remodeling (Figure 7B). Remains of the cartilage matrix are preserved inside some of the trabeculae. Thoracic ribs demonstrate asymmetrical growth, as mentioned for several basilosaurid taxa (Buffrénil et al., 1990; Houssaye et al., 2015), in a way that the medullar area shifted to the medial side of the rib (Supplementary Figure S5), whereas layers of periosteal cortex formed a pachyostotic swelling on the lateral and posterior sides.

3.3.3 Scapula (NMNH-P CS 46/9)

The cortex is composed of pseudolamellar bone tissue with simple vascular canals and scarce primary osteons, oriented at

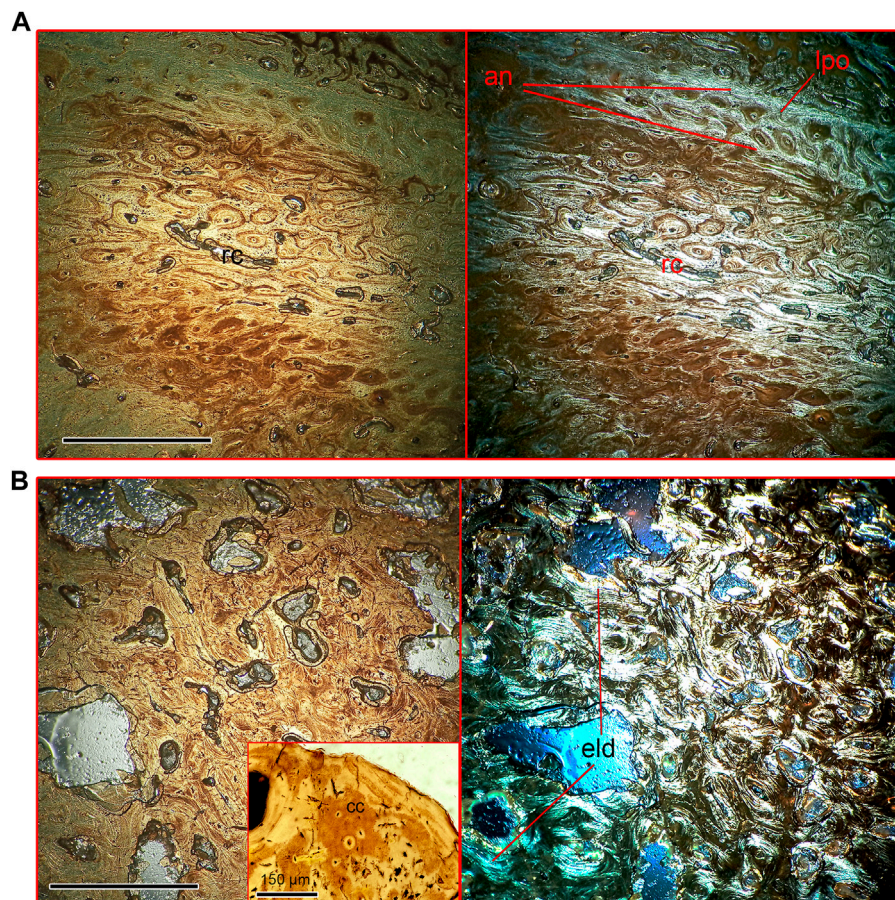


FIGURE 7

Microanatomical structure of the thoracic rib (Nahirne specimen, NMNH-P CS 52) of *Basilotritus* sp. **(A)** Natural (left) and polarized (right) microscopical views on the rib cortex. **(B)** Natural (left) and polarized (right) microscopical views on the medullar area. Trabeculae with calcified cartilage are shown in the inset. Abbreviations: an, annuli; cc, calcified cartilage; eld, endosteal lamellar deposits; lpo, line of primary osteons; rc, resorption cavities. All scale bars except one for the inset are 0.5 mm.

different angles (Figure 8A). The medullar area is filled by thin trabeculae with moderate endosteal lamellar deposits and secondary osteons (Figure 8B). Endosteal lamellar bone is absent on the walls of some trabeculae, showing the presence of Howship's lacunae (Gray et al., 2007). Generally, the scapula is pachyostotic due to the presence considerably thickened cortex at least at lateral side (medial is eroded) (Supplementary Figure S2K).

3.3.4 Innominate (NMNH-P CS 51/3)

The cortex is composed of woven bone and numerous primary and secondary osteons. Irregular resorption cavities penetrate the cortex (Figure 9A). The bone histology of the medullar area is similar to that in the scapula (Figure 8B).

3.3.5 Mandible (NMNH-P CS 41/8)

The cortex of the ventral part of the horizontal ramus of the mandible is composed of woven bone tissue with simple vascular canals. There are five discontinuous annuli formed by lamellar bone deposits in the depth of the cortex (Figure 9B).

4 Discussion

Skeletal microanatomy of many aquatic mammals follows a single adaptive strategy; however, an opposite situation is equally common: the postcranial skeleton of many secondary aquatic tetrapods in several evolutionary lineages is a mosaic of bone structure types (Ricqlès and De Buffrénil, 2001; Houssaye et al., 2016; Houssaye and Buffrénil, 2021). Such a diversity is sometimes associated with an early stage of adaptation to an aquatic environment, or, in other cases, with such tetrapods living in coastal waters. For example, the postcranial skeleton of an extant *Dugong dugong* (Sirenia, Dugongidae) includes pachyosteosclerotic/osteosclerotic ribs, forelimb bones and anterior thoracic vertebrae, whereas the rest of the vertebral column has a cancellous structure (Buffrénil and Schoevaert, 1989). A similar mix is observed in skeletons of the Oligocene semiaquatic mammals *Behemotops katsuiei* and *Ashroa laticosta* (Desmostylia), which have osteosclerotic or pachyosteosclerotic ribs and limb bones combined with cancellous vertebrae (Hayashi et al., 2013). Also, diversification of postcranial bone microstructure is documented for some sauropterygians (Cruickshank et al., 1996; Street and O'Keefe,

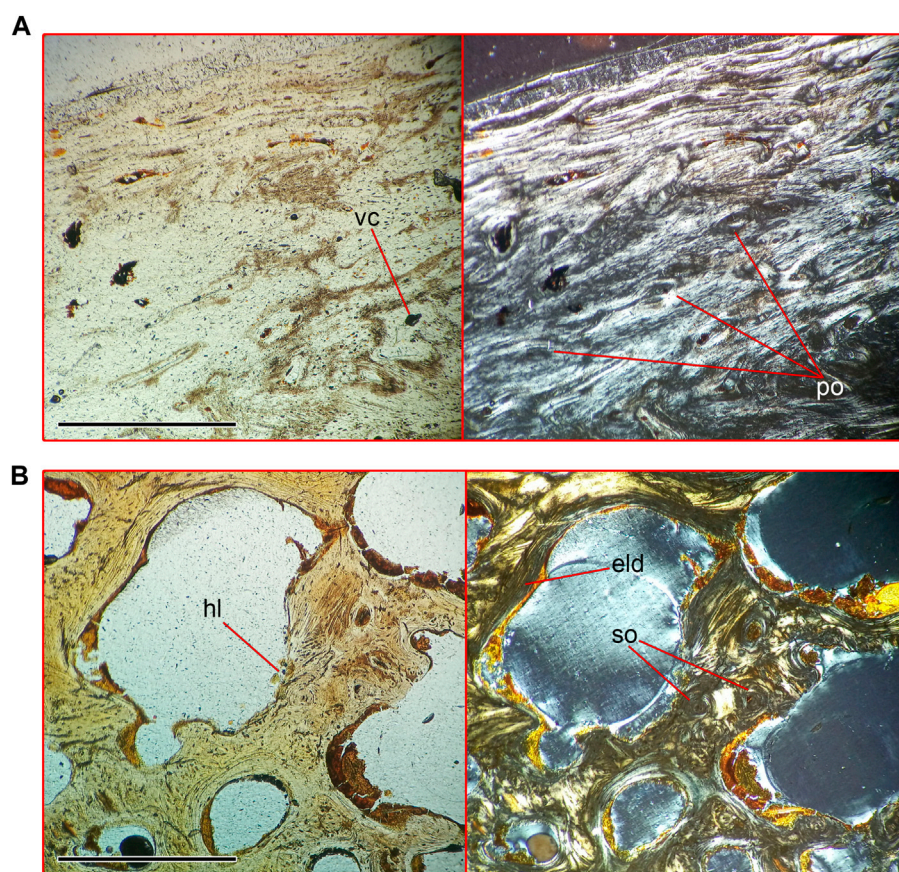


FIGURE 8

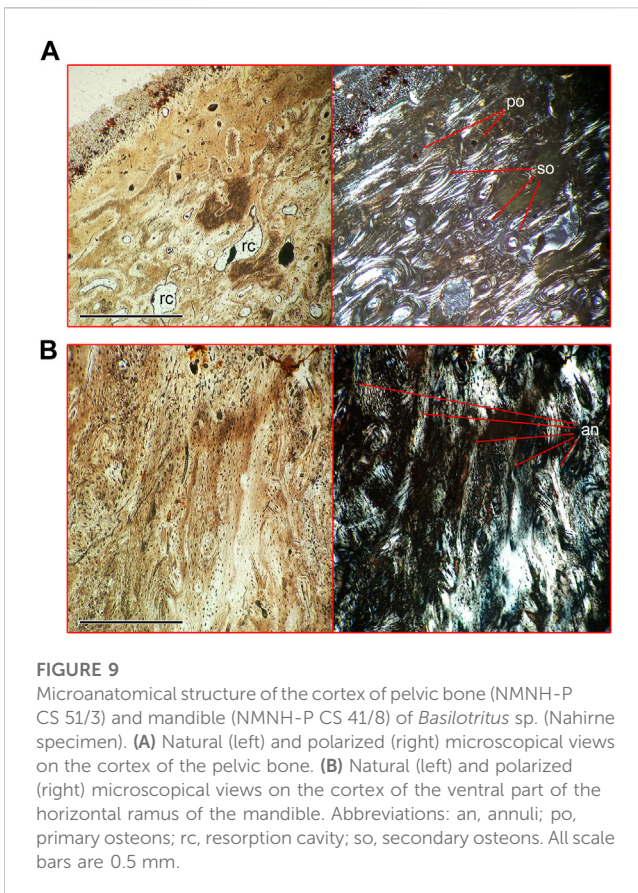
Microanatomical structure of the posterior portion of the scapular blade (Nahirne specimen, NMNH-P CS 46/9) of *Basilotritus* sp. (A) Natural (left) and polarized (right) microscopical views on the cortex of the scapula. (B) Natural (left) and polarized (right) microscopical views on the medullar area on the scapula. Abbreviations: eld, endosteal lamellar deposits; hl, Howship's lacunae; po, primary osteons; vc, vascular canal. All scale bars are 0.5 mm.

2010), which have dense ribs and gastralria. Efficient buoyancy control through loading of the skeleton has been proposed as a functional interpretation of bone mass increase in the mentioned aquatic tetrapods. However, there are some groups of secondary aquatic tetrapods showing a different type of skeletal adaptations: all parts of the postcranial skeleton of the same individual display a uniform type of microstructure. Well documented examples of such aquatic tetrapods are crown cetaceans (Ricqlès and De Buffrénil, 2001) and most of the ichthyosaurs (Sander, 2021). The whole postcranial skeleton of these pelagic swimmers is composed of cancellous, even osteoporotic-like bone tissue (in case of the many crown cetaceans, e.g., dolphins). Aquatic tetrapods which have an opposite microstructure condition are known (although quite rare): the recovered postcranial skeletal parts of such animals are osteosclerotic or pachyosteosclerotic. These include several mammals represented by cetaceans—mysticetes of the family Cetotheriidae, an odontocete *Pachyacanthus* and a true seal *Nannophoca* from the Miocene (Gol'din et al., 2014a; Dewaele et al., 2022) and reptiles represented by Permian mesosaurs and Cretaceous stem-ophidiomorphs (Houssaye, 2013; Houssaye et al., 2016). Unusual structural homogeneity and extremely high compactness of almost every bone in their skeletons were interpreted as an adaptation to hypersaline conditions, in case of

cetaceans (Dewaele et al., 2022), or aspects of aquatic locomotion, in case of some marine reptiles (Houssaye et al., 2016).

The results of this study show that the basilosaurid whale *Basilotritus* has diverse bone tissues in the postcranial skeleton. It includes pachyosteosclerotic (thoracic ribs, posterior thoracic and lumbar vertebrae), pachyostotic (scapulae, pelvis), osteosclerotic (humerus) and cancellous (cervical and caudal vertebrae) elements. Microstructure of cortex layering is different depending on the bone. For example, in ribs of the Nahirne specimen the cortical layers are divided by numerous annuli, whereas in lumbar vertebra of the same specimen (which were found in close association with the ribs and undoubtedly belong to the same individual) these layers are separated by longitudinal vascular canals organized in circular rows, and only a single annulus is seen there.

Due to this microstructural diversity, the skeleton of *Basilotritus* is a mosaic of light and heavy bones. Diversity of bone tissues, although less studied, is known for other basilosaurids as well as for geologically older semi-aquatic archaeocetes (Houssaye et al., 2015). The heaviest bones are concentrated in the posterior thoracic and lumbar regions of the vertebral column. Heavy vertebrae of these regions compose a significant part of the axial skeleton (the number of thoracic vertebrae is estimated as 12 for *Basilotritus* (Gol'din and Zvonok, 2013) and of lumbar vertebrae as around 10 for the unnamed Bartonian



basilosaurid from Peru MUSM 1443 (Uhen et al., 2011)) and therefore they would form a ballast similar to that of sirenians and some other secondary aquatic mammals (Buffrénil and Schoevaert, 1989; Hayashi et al., 2013; Dewaele et al., 2022). However, a few dense bones are also situated in the ventral parts of the skeleton, including swollen distal ends of thoracic ribs, distal end of the humerus and pachyostotic pelvis, therefore producing an additional ballast on the ventral side of the body. This weight distribution is more complex than in skeletons of other known basilosaurids which show only ventral (swollen ribs) ballast (Kellogg, 1936; Uhen, 2004; Martínez-Cáceres et al., 2017). Concentration of dense bones in two areas may help to enhance buoyancy control for an elongated body of an epipelagic predator (Gol'din et al., 2014b). In overall, such a pattern is different from other well-studied Eocene cetaceans like *Dorudon atrox* and *Cynthiacetus peruvianus* (Uhen, 2004; Martínez-Cáceres et al., 2017) but can be similar to some least studied specimens including MUSM 1443 and *Antaeocetus aithai* (Uhen et al., 2011; Gingerich et al., 2022). The presence of a thick, intensively vascularized cortex in vertebrae seems to be an autapomorphy (or a synapomorphy for a clade of basal Pelagiceti). Pachyostosis of an innominate may be also an autapomorphy. Interestingly, the only previous study of the inner microstructure of the innominate of an Eocene cetacean (a member of the family Protocetidae) revealed that its bone was composed of cancellous bone tissue (Hautier et al., 2014). However, pachyosteosclerotic ribs are shared with most lineages of early Pelagiceti (Buffrénil et al., 1990; Houssaye et al., 2015; Muizon et al., 2019) and an osteosclerotic humerus is a plesiomorphic condition for cetaceans, although its density seems to be lower

than in semiaquatic Pakicetidae and Protocetidae (Madar, 2007; Houssaye et al., 2015). There are several middle Eocene cetaceans sharing pachyosteosclerotic skeleton; those are globally distributed and show body size disparity: large representatives designated as *Basilotritus*, *Pachycetus* and *Platyosphys* are known from Europe (Fedorovsky, 1912; Gol'din and Zvonok, 2013; van Vliet et al., 2020), whereas smaller forms include *Antaeocetus aithai* and several “*Eocetus*” specimens from the North Africa (Gingerich et al., 2022), “*Basilotritus*” *wardii* and similar forms from North America and MUSM 1443 from South America (Uhen, 1999; Uhen et al., 2011). However, little is known about details of anatomy, microanatomy, diversity and phylogenetic relationships of these cetaceans.

Another interpretation, which cannot be ruled out, is that the difference in microstructure between bones can be due to different growth rates or development patterns, when the primary type of bone inner structure changes during the ontogeny, as in the case described by Wiffen et al. (1995) when the juvenile individuals of a Late Cretaceous plesiosaur show pachyosteosclerosis while adults have osteoporotic-like structures. Therefore, the long-growing or positively allometric bones (as for extant cetaceans (Galatius, 2005)), are pachyosteosclerotic (e.g., thoracic and lumbar vertebrae and ribs) or pachyostotic (scapula), whereas the bones in which growth ceases early—cervical and caudal vertebrae—are cancellous. The vascular system of the pachyosteosclerotic vertebral cortex, organized as numerous longitudinal vascular canals arranged in circular rows, may be associated with a slow growth rate, as it has been suggested for the mosasauroid *Clidastes propython* (Houssaye and Bardet, 2012). This is an additional indicator of different growth rates for different bones in the skeleton of *Basilotritus*. Also, contrary to the example described by Wiffen et al. (1995), *Basilotritus uheni* retains numerous pachyosteosclerotic bones in the adult state, as seen from the anatomy of NMNH-P OF-2096. However, an interpretation based on ontogenetic changes is limited for this study, since the specimens examined here could belong to different species with different ontogenetic trajectories.

Moreover, cortical bone tissue of vertebrae and ribs of *Basilotritus* displays numerous signs of intensive resorption and remodeling and, at the same time, a complex vascularization pattern forming a dense vascular system. Numerous resorption cavities may be an evidence of use of the axial skeleton not only for buoyancy control but also as a depot of nutrients or ions, e.g., of calcium and phosphorous, at certain ontogenetic stages or depending on mineral availability in the environment (Cowan et al., 1968; George et al., 2016). However, this hypothesis could only be tested through the study of a larger number of specimens from a single species and with different ontogenetic stages. Interestingly, the presence of numerous resorption cavities in bones distinguishes the pachyosteosclerotic skeleton of *Basilotritus* from the pachyosteosclerotic bones of several Miocene marine mammals, whose bones are roughly uniform in microstructure (Dewaele et al., 2022). Different evolutionary mechanisms may have been involved in developing these superficially similar morphotypes.

5 Conclusion

Several, globally distributed basal members of Pelagiceti (fully aquatic cetaceans) from the middle Eocene share a vertebral

morphotype, characterized by elongated and pachyosteosclerotic thoracics and lumbar. Among them, specimens from late middle Eocene deposits of Ukraine have been assigned to the genus *Basilotritus*. Close examination of inner structure of bones of three main specimens reveals a complex pattern of bone tissue distribution across various parts of the skeleton. The postcranial skeleton of *Basilotritus* is composed of bones having different growth rates, as seen from different layering and vascularization in ribs and vertebrae. Their skeleton shows an advanced system of ballast distribution with heavy bones concentrated in the dorsal and the ventral areas. Such a system distinguishes *Basilotritus* from previously studied basilosaurids which have heavy bones only in the rib cage. Combination of heavy vascularization and intensive resorption and reconstruction may be an evidence for a possible function of the skeleton for calcium and phosphorus recycling.

Data availability statement

The original contributions presented in the study are included in the article/[Supplementary Material](#), further inquiries can be directed to the corresponding authors.

Author contributions

SD and PG. planned the study; SD and RT. collected data; PG led the analysis; SD analyzed data; SD and PG wrote the initial manuscript draft with input from all the authors. All authors contributed to the manuscript and approved the final version. All authors listed have made a substantial, direct, and intellectual contribution to the work and approved it for publication.

Funding

The work by SD and PG was funded by the National Research Foundation of Ukraine, grant 2020.02/0247 “Integration of

mammalian organism as a proxy of stability at aquatic and aerial life (as illustrated by skeleton traits)”.

Acknowledgments

We sincerely thank Olga Vakulenko and Oleksandr Kovalchuk who provided materials under their care; Igor Chernikov who donated materials for this study; Michel Laurin and Jordan Gônet for providing the BoneProfiler software; Vivian de Buffrénil and the anonymous reviewer 2 for reviewing the paper, Olivier Lambert, Graciela Piñeiro and Mark D. Uhen for discussing the draft of the manuscript.

Conflict of interest

The authors declare that the research was conducted in the absence of any commercial or financial relationships that could be construed as a potential conflict of interest.

The reviewer VDB declared a past co-authorship with the author PG'd to the handling editor TBC.

Publisher's note

All claims expressed in this article are solely those of the authors and do not necessarily represent those of their affiliated organizations, or those of the publisher, the editors and the reviewers. Any product that may be evaluated in this article, or claim that may be made by its manufacturer, is not guaranteed or endorsed by the publisher.

Supplementary material

The Supplementary Material for this article can be found online at: <https://www.frontiersin.org/articles/10.3389/feart.2023.1168681/full#supplementary-material>

References

- Buffrénil, V., De Ricqlès, A., Ray, C. E., and Domning, D. P. (1990). Bone histology of the ribs of the archaeocetes (Mammalia: Cetacea). *J. Vertebr. Paleontol.* 10, 455–466. doi:10.1080/02724634.1990.10011828
- Buffrénil, V., and Schoevaert, D. (1988). On how the periosteal bone of the delphinid humerus becomes cancellous: Ontogeny of a histological specialization. *J. Morphol.* 198, 149–164. doi:10.1002/jmor.1051980203
- Buffrénil, V., Canoville, A., D'Anastasio, R., and Domning, D. P. (2010). Evolution of sirenian pachyosteosclerosis, a model-case for the study of bone structure in aquatic tetrapods. *J. Mamm. Evol.* 17, 101–120. doi:10.1007/s10914-010-9130-1
- Buffrénil, V. de, and Mazin, J. M. (1990). Bone histology of the ichthyosaurs: Comparative data and functional interpretation. *Paleobiology* 16, 435–447. doi:10.1017/S0094837300010174
- Buffrénil, V., and Quilhac, A. (2021). “Bone tissue types,” in *Vertebrate skeletal histology and paleohistology*. Editors V. de Buffrénil, A. de Ricqlès, L. Zylberberg, and K. Padian (Florida, United States: CRC Press), 148–176. doi:10.1201/9781351189590-36
- Buffrénil, V., and Schoevaert, D. (1989). Données quantitatives et observations histologiques sur la pachyostose du squelette du dugong, *Dugong dugon* (Müller) (Sirenia, Dugongidae). *Can. J. Zool.* 67, 2107–2119. doi:10.1139/z89-300
- Cowan, R. L., Hartsook, E. W., and Whelan, J. B. (1968). Calcium-strontium metabolism in white tailed deer as related to age and antler growth. *Proc. Soc. Exp. Biol. Med.* 129, 733–737. doi:10.3181/00379727-129-33412
- Cruikshank, A. R. I., Martill, D. M., and Noè, L. F. (1996). A pliosaur (Reptilia, Sauropterygia) exhibiting pachyostosis from the middle jurassic of England. *J. Geol. Soc. Lond.* 153, 873–879. doi:10.1144/gsjgs.153.6.0873
- Davydenko, S., Shevchenko, T., Ryabokon, T., Tretiakov, R., and Gol'din, P. (2021). A giant Eocene whale from Ukraine uncovers early cetacean adaptations to the fully aquatic life. *Evol. Biol.* 48, 67–80. doi:10.1007/s11692-020-09524-8
- Dewaele, L., Gol'din, P., Marx, F. G., Lambert, O., Laurin, M., Obadã, T., et al. (2022). Hypersalinity drives convergent bone mass increases in Miocene marine mammals from the Paratethys. *Curr. Biol.* 32, 248–255.e2. doi:10.1016/j.cub.2021.10.065
- Dewaele, L., Lambert, O., Laurin, M., De Kock, T., Louwyte, S., and de Buffrénil, V. (2019). Generalized osteosclerotic condition in the skeleton of *Nanophoca vitulinoides*, a dwarf seal from the Miocene of Belgium. *J. Mamm. Evol.* 26, 517–543. doi:10.1007/s10914-018-9438-9
- Fedorovsky, A. (1912). A record of a fossil cetacean in Zmieiv uyezd of Kharkov government. *Tr. Obs. Prir. Kharkovskogo Univeristeta* 14, 253–287.
- Francillon-Vieillot, H., de Buffrénil, V., Castanet, J., Géraudie, J., Meunier, F. J., Sire, J. Y., et al. (1990). “Microstructure and mineralization of vertebrate skeletal tissues,” in *Skeletal biomineralization: Patterns, processes and evolutionary trends*. Editor J. G. Carter (Malabar, Florida: Van Nostrand Reinhold), 175–234. doi:10.1029/sc005p0175

- Galatius, A., and Kinze, C. C. (2003). Ankylosis patterns in the postcranial skeleton and hyoid bones of the harbour porpoise (*Phocoena phocoena*) in the Baltic and North Sea. *Can. J. Zool.* 81, 1851–1861. doi:10.1139/z03-181
- Galatius, A. (2005). Sexually dimorphic proportions of the harbour porpoise (*Phocoena phocoena*) skeleton. *J. Anat.* 206, 141–154. doi:10.1111/j.1469-7580.2005.00381.x
- George, J. C., Stimmelmayer, R., Suydam, R., Usip, S., Givens, G., Sformo, T., et al. (2016). Severe bone loss as part of the life history strategy of bowhead whales. *PLoS One* 11, 01567533–e156814. doi:10.1371/journal.pone.0156753
- Gingerich, P. D., Amame, A., and Zouhri, S. (2022). Skull and partial skeleton of a new pachycetinae genus (Cetacea, Basilosauridae) from the Aridal Formation, Bartonian middle Eocene, of southwestern Morocco. *PLoS One* 17 (10), e0276110. doi:10.1371/journal.pone.0276110
- Girondot, M., and Laurin, M. (2003). Bone profiler: A tool to quantify, model, and statistically compare bone-section compactness profiles. *J. Vertebr. Paleontol.* 23, 458–461. doi:10.1671/0272-4634(2003)023[0458:BPATTQ]2.0.CO;2
- Gol'din, P., Startsev, D., and Krakhmalnaya, T. (2014a). The anatomy of the late miocene baleen whale *Cetotherium riabinini* from Ukraine. *Acta Palaeontol. Pol.* 59, 795–814. doi:10.4202/app.2012.0107
- Gol'din, P., and Zvonok, E. (2013). *Basilotritus uheni*, a new cetacean (Cetacea, Basilosauridae) from the late middle Eocene of eastern Europe. *J. Paleontol.* 87, 264–268. doi:10.1666/12-080r.1
- Gol'din, P., Zvonok, E., Rekovets, L., Kovalchuk, A., and Krakhmalnaya, T. (2014b). *Basilotritus* (Cetacea: Pelagiceti) from the Eocene of Nagornoye (Ukraine): New data on anatomy, ontogeny and feeding of early basilosaurids. *Comptes Rendus - Palevol* 13, 267–276. doi:10.1016/j.crpv.2013.11.002
- Gray, N. M., Kainec, K., Madar, S., Tomko, L., and Wolfe, S. (2007). Sink or swim? Bone density as a mechanism for buoyancy control in early cetaceans. *Anat. Rec.* 290, 638–653. doi:10.1002/ar.20533
- Hautier, L., Sarr, R., Lihoreau, F., Tabuce, R., and Marwan Hameh, P. (2014). First record of the family Protocetidae in the lutetian of Senegal (west Africa). *Palaeovertebrata* 38. doi:10.18563/pv.38.2.e2
- Hayashi, S., Houssaye, A., Nakajima, Y., Chiba, K., Ando, T., Sawamura, H., et al. (2013). Bone inner structure suggests increasing aquatic adaptations in Desmostylia (Mammalia, Afrotheria). *PLoS One* 8, 591466–e59235. doi:10.1371/journal.pone.0059146
- Houssaye, A., and Bardet, N. (2012). Rib and vertebral micro-anatomical characteristics of hypodolpvid mosasaurids. *Lethaia* 45, 200–209. doi:10.1111/j.1502-3931.2011.00273.x
- Houssaye, A., and de Buffrénil, V. (2021). “Bone histology and the adaptation to aquatic life in tetrapods,” in *Vertebrate skeletal histology and paleohistology*. Editors V. de Buffrénil, A. de Ricqlès, L. Zylberberg, and K. Padian (Florida, United States: CRC Press), 744–756. doi:10.1201/9781351189590-36
- Houssaye, A., Martin Sander, P., and Klein, N. (2016). Adaptive patterns in aquatic amniote bone microanatomy - more complex than previously thought. *Integr. Comp. Biol.* 56, 1349–1369. doi:10.1093/icb/icw120
- Houssaye, A. (2013). Palaeoecological and morphofunctional interpretation of bone mass increase: An example in Late Cretaceous shallow marine squamates. *Biol. Rev.* 88, 117–139. doi:10.1111/j.1469-185X.2012.00243.x
- Houssaye, A., Scheyer, T. M., Kolb, C., Fischer, V., and Martin Sander, P. (2014). A new look at ichthyosaur long bone microanatomy and histology: Implications for their adaptation to an aquatic life. *PLoS One* 9, 956377–e95710. doi:10.1371/journal.pone.0095637
- Houssaye, A., Tafforeau, P., De Muizon, C., and Gingerich, P. D. (2015). Transition of Eocene whales from land to sea: Evidence from bone microstructure. *PLoS One* 10, e0118409–e0118428. doi:10.1371/journal.pone.0118409
- Kato, H. (1988). Ossification pattern of the vertebral epiphyses in the southern minke whale. *Sci. Rep. Whales Res. Inst. Tokyo* 39, 11–20.
- Kellogg, R. (1936). *A review of the archaeoceti*. Washington, USA: Carnegie Institution of Washington. doi:10.2307/1374291
- Klein, N., Sander, P. M., Krahl, A., Scheyer, T. M., and Houssaye, A. (2016). Diverse aquatic adaptations in *Nothosaurus* spp. (Sauropterygia) - inferences from humeral histology and microanatomy. *PLoS One* 11, 0158448–e158530. doi:10.1371/journal.pone.0158448
- Klevezal, G. A. (1996). *Recording structures of mammals: Determination of age and reconstruction of life history*. Berlin, Germany: ResearchGate. doi:10.1201/9780203741146
- Lamm, E. T. (2013). Preparation and sectioning of specimens. *Bone Histol. Foss. Tetrapods Adv. Methods, Anal. Interpret.* 2013, 55–160.
- Madar, S. I. (2007). The postcranial skeleton of early Eocene pakicetid cetaceans. *J. Paleontol.* 81, 176–200. doi:10.1666/0022-3360(2007)81[176:TPSOEE]2.0.CO;2
- Martínez-Cáceres, M., Lambert, O., and de Muizon, C. (2017). The anatomy and phylogenetic affinities of *Cynthiacetus peruvianus*, a large *Dorudon*-like basilosaurid (Cetacea, Mammalia) from the late Eocene of Peru. *Geodiversitas* 39, 7–163. doi:10.5252/g2017n1a1
- Medixant (2021). RadiAnt DICOM Viewer. Version 2021. Available at: <https://www.radiantviewer.com>.
- Moran, M. M., Bajpai, S., George, J. C., Suydam, R., Usip, S., and Thewissen, J. G. M. (2015). Intervertebral and epiphyseal fusion in the postnatal ontogeny of cetaceans and terrestrial mammals. *J. Mamm. Evol.* 22, 93–109. doi:10.1007/s10914-014-9256-7
- Muizon, C., Bianucci, G., Martínez-Cáceres, M., and Lambert, O. (2019). *Mystacodon selenensis*, the earliest known toothed mysticete (cetacea, mammalia) from the late Eocene of Peru: Anatomy, phylogeny, and feeding adaptations. *Geodiversitas* 41, 401. doi:10.5252/geodiversitas2019v41a11
- Núñez Demarco, P., Meneghel, M., Laurin, M., and Piñeiro, G. (2018). Was *mesosaurus* a fully aquatic reptile? *Front. Ecol. Evol.* 6. doi:10.3389/fevo.2018.00109
- Ricqlès, de A., and De Buffrénil, V. (2001). “Bone histology, heterochronies and the return of tetrapods to life in water: Where are we?,” in *Secondary adaptation of tetrapods to life in water* (Munich, Germany: Verlag Friedrich Pfeil), 289–310.
- Sander, P. M. (2021). “Ichthyosauria,” in *Vertebrate skeletal histology and paleohistology*. Editors V. de Buffrénil, A. de Ricqlès, L. Zylberberg, and K. Padian (Boca Raton and London: CRC Press), 458–465.
- Scheyer, T. M., Danilov, I. G., Sukhanov, V. B., and Syromyatnikova, E. V. (2014). The shell bone histology of fossil and extant marine turtles revisited. *Biol. J. Linn. Soc.* 112, 701–718. doi:10.1111/bij.12265
- Street, H. P., and O'Keefe, F. R. (2010). Evidence of pachyostosis in the cryptocleidoid plesiosaur *Tatenectes laramiensis* from the Sundance Formation of Wyoming. *J. Vertebr. Paleontol.* 30, 1279–1282. doi:10.1080/02724634.2010.483543
- Thewissen, J. G. M., Cooper, L. N., Clementz, M. T., Bajpai, S., and Tiwari, B. N. (2007). Whales originated from aquatic artiodactyls in the Eocene epoch of India. *Nature* 450, 1190–1194. doi:10.1038/nature06343
- Uhen, M. D. (2004). Form, function, and anatomy of *Dorudon atrox* (mammalia, cetacea): An archaeocete from the middle to late Eocene of Egypt. *Pap. Paleontol.* 34, 1–238.
- Uhen, M. D. (1999). New species of protocetid archaeocete whale, *Eocetus wardii* (Mammalia: Cetacea) from the middle Eocene of North Carolina. *J. Paleontol.* 73, 512–528. doi:10.1017/S002233600002802X
- Uhen, M. D., Pyenson, N. D., De Vries, T. J., Urbina, M., and Renne, P. R. (2011). New middle Eocene whales from the pisco basin of Peru. *J. Paleontol.* 85, 955–969. doi:10.1666/10-162.1
- Van Benden, P. J. (1883). Sur quelques ossements de cétacés fossiles, recueillis dans des couches phosphatées entre l'Elbe et le Weser. *Bull. L'Academie Sci. lettres B.-art.* 6, 27–33.
- van Vliet, H. J., Bosselaers, M., Schouten, S., Post, K., and Reumer, J. W. F. (2022). Eocene cetaceans from the Belgian-Dutch coastal waters. *Deinsea* 20, 1–34.
- van Vliet, H. J., Bosselaers, M., Vahldiek, B., Paymans, T., and Verheijen, I. (2020). Eocene cetaceans from the helmstedt region, Germany, with some remarks on *Platysphys*, *Basilotritus* and *Pachycetus*. *Cainozoic Res.* 20, 121–148.
- Wiffen, J., de Buffrénil, V., de Ricqlès, A., and Mazin, J. M. (1995). Ontogenetic evolution of bone structure in late cretaceous plesiosauria from New Zealand. *Geobios* 28, 625–640. doi:10.1016/S0016-6995(95)80216-9